Partial Shade Stress Test for Thin-Film Photovoltaic Modules

Preprint

Timothy J. Silverman, Michael G. Deceglie, Chris Deline, and Sarah Kurtz
National Renewable Energy Laboratory

Presented at SPIE Optics + Photonics
San Diego, California
August 9–13, 2015

NREL is a national laboratory of the U.S. Department of Energy
Office of Energy Efficiency & Renewable Energy
Operated by the Alliance for Sustainable Energy, LLC

This report is available at no cost from the National Renewable Energy Laboratory (NREL) at www.nrel.gov/publications.

Conference Paper
NREL/CP-5J00-64456
September 2015

Contract No. DE-AC36-08GO28308

NOTICE

This report is available at no cost from the National Renewable Energy Laboratory (NREL) at www.nrel.gov/publications.

Available electronically at SciTech Connect http:/www.osti.gov/scitech

Available for a processing fee to U.S. Department of Energy and its contractors, in paper, from:

U.S. Department of Energy
Office of Scientific and Technical Information
P.O. Box 62
Oak Ridge, TN 37831-0062
OSTI http://www.osti.gov
Phone: 865.576.8401
Fax: 865.576.5728
Email: reports@osti.gov

Available for sale to the public, in paper, from:

U.S. Department of Commerce
National Technical Information Service
5301 Shawnee Road
Alexandria, VA 22312
NTIS http://www.ntis.gov
Phone: 800.553.6847 or 703.605.6000
Fax: 703.605.6900
Email: orders@ntis.gov

Cover Photos by Dennis Schroeder: (left to right) NREL 26173, NREL 18302, NREL 19758, NREL 29642, NREL 19795.

NREL prints on paper that contains recycled content.

Partial shade stress test for thin-film photovoltaic modules

Timothy J Silverman*, Michael G. Deceglie, Chris Deline and Sarah Kurtz

National Renewable Energy Laboratory, Golden, Colorado, United States

ABSTRACT

Partial shade of monolithic thin-film PV modules can cause reverse-bias conditions leading to permanent damage. In this work, we introduce a partial shade stress test for thin-film PV modules that quantifies permanent performance loss. The test reproduces shading and loading conditions that may occur in the field. It accounts for reversible light-induced performance changes and for the effects of light-enhanced reverse breakdown. We simulated the test procedure using a computer model that predicts the local voltage, current and temperature stress resulting from partial shade. We also performed the test on three commercial module types. Each module type we tested suffered permanent damage during masked flash testing totaling < 2 s of light exposure. During the subsequent stress test these module types lost 4%–11% in P_{mp} due to widespread formation of new shunts. One module type showed a substantial worsening of the P_{mp} loss upon light stabilization, underscoring the importance of this practice for proper quantification of damage.

Keywords: photovoltaics, reliability, photovoltaic modules, thin film

1. INTRODUCTION

Monolithic thin-film PV modules often contain more than 100 series-connected cells. This serial interconnection means that each cell must pass the same current. When a cell is shaded, it can only pass photocurrent from the rest of the string by moving into reverse bias. Series-connected monolithic modules are often protected by a single bypass diode, so even when a mask covers multiple cells, the large number of still-illuminated cells provide the driving force for current flow in the masked cells. This can cause permanent damage due to the strong electric field, large current density and high dissipated power density associated with reverse-bias operation. Cells are frequently shaded during service by structures, animals, soiling, and other obstructions that may be distant or directly on the module surface.

The present standard partial shade stress test, namely the hot spot endurance test in the design qualification test for thin-film PV modules, is designed to detect problems such as solder melting and encapsulant deterioration.[1] Modules pass the hot spot endurance test if they maintain their insulation resistance and lack major visual defects. As such, it is an effective test for problems that may lead to fire or safety risk, however a module can pass regardless of how much performance loss has occurred. Revisions to this test, proposed by others as part of edition 3 of IEC 61215, require that a passing module produce a functional I-V curve after stress, but still with no requirement on retention of electrical performance.

2. CONSIDERATIONS FOR A QUANTITATIVE PARTIAL SHADE TEST

In this work we introduce a test procedure that quantifies a module's robustness to partial shade stress. The procedure can be used as a starting point for comparative tests that help guide technology development and for qualification tests to screen for faulty product designs. A test procedure for quantifying robustness to partial shade stress must move beyond the standard test with careful quantification of the change in module performance resulting from stress and with stress conditions that are based upon realistic service. In this work we show a test procedure that meets these requirements.

In this work, we focus on monolithic CIGS modules containing a single series string of cells. This is the typical configuration of most CIGS products. We expect the procedure to readily adapt to other monolithic thin-film PV module technologies such as CdTe.

* timothy.silverman@nrel.gov

The procedure is performed in two stages. During the mask sizing stage, the size of the mask to be used during stress is determined using I-V measurements under pulsed illumination. During the stress stage, a modified version of the mask is applied repeatedly during continuous illumination with the module passing its unshaded, operating-temperature I_{mp}. Light I-V curves collected for evaluating performance loss are done so after light stabilization, sometimes called light soaking.

2.1 Mask sizing

The standardized hot spot endurance test includes a procedure for determining the worst-case mask size, where the worst case is defined as the maximum total dissipation of power in the module. The standard acknowledges that this procedure, which is performed before the phase of the test intended to apply stress, can itself result in permanent damage. Others have proposed changes to the standard that include a recommendation to perform this process on a pulsed simulator to minimize this damage. We have observed that this practice still causes permanent damage. To minimize the effect of this damage on the results of both phases of the test, we introduce two new practices: the use of a shrinking mask during sizing and of a previously unstressed module during stress. We also use a slightly different definition of "worst case" to define the mask that is used during stress.

On a single module, applying a large mask permits only a small amount of current to flow, even in short-circuit conditions. This limits the dissipation of power in the masked cells, often limiting the associated damage. The forward voltage of the illuminated cells is also divided among a larger number of masked cells, reducing the stress associated with strong electric field. Therefore, we begin the mask sizing procedure with a large mask and progressively shrink it until the size of the mask to be used during stress is identified. This reduces the likelihood that damage caused by a small mask early in the procedure might affect the final result of the procedure.

We have observed that, even using a shrinking mask and a pulsed simulator, some permanent damage still results from a series of masked flashes, as shown in Figure 4. This damage takes the form of shunting and, if the shunted cells are illuminated while another area of the module is masked, this shunting reduces the forward voltage available to reverse-bias the masked cells. Therefore, we perform the mask sizing test in only one area of the module to prevent this damage from affecting the results. Damage sustained during the mask sizing procedure has the potential to affect the outcome of subsequent tests. We have adopted the practice of using a previously unstressed module for the stress stage of the test. However, with careful planning it may be possible to account for these effects and to perform the entire test with a single module.

The stress phase of the test entails multiple applications of the critical mask, each in a different area. In this case the critical mask is not the one that maximizes power dissipation in the module. Instead, the critical mask is the largest one that results in nearly the maximum possible dissipated power per cell. A single-cell mask would maximize the power dissipation per cell, but such a narrow mask is not practical. Instead, we use masks that achieve ∼90% of this power dissipation per cell, but on many cells at once. The method for determining the critical mask size is detailed in Section 3.2.

2.2 Partial shade stress

Obstructions to modules in service do not block 100% of the incident light. Even with intentional masking, some light can always reach the masked cells because there is normally ~ 4 mm of transparent packaging material between the obstruction and the cells. This can lead to a large fractional difference in the amount of light allowed to reach cells behind slightly different masks that are intended to be opaque. For example, small changes to the size of any air gap between the mask and the module or to the reflectivity of the back side of the mask may cause wide variation in the small amount of light reaching the masked cells.

At low levels of illumination, the exact amount of light reaching a masked CIGS cell plays a critical role in reverse breakdown. This is due to the phenomenon of light-enhanced reverse breakdown (LERB), which causes the reverse breakdown voltage of some CIGS cells to be greatly reduced during exposure to light. The effect has been demonstrated on laboratory and flexible-substrate cells[2–4] and we have recently demonstrated it on a commercial monolithic CIGS sample.[5] The physical origin of the effect is still under investigation and a mechanism has recently been proposed as part of an effort to build a physical model of a cell with LERB.[6] The dependence of breakdown voltage on light intensity is most sensitive at low intensities, below ~ 100 Wm^{-2}.[2,4]

To more accurately represent real shadows and to eliminate the wide range in the intensity of light reaching cells behind non-ideal totally opaque masks, we perform partial shade testing using a 90% opaque (10% transmitting) mask. Outdoors, under clear-sky conditions, a shadow cast by a distant object may block approximately 90% of incident light.

When a shadow covers only part of a cell, current flows preferentially in the illuminated portion of that cell.[5,7] This is especially pronounced in modules that exhibit LERB, but still occurs in modules with light-independent reverse breakdown due in part to the temperature dependence of the reverse characteristic. This current crowding effect causes high dissipation of heat in the illuminated portion of the cells and, combined with the incident light, leads to high temperature in these areas. This kind of current crowding does not occur when the entire length of the cell is masked, so in a uniform module the peak temperature is substantially lower under these conditions.[5] A partial-coverage mask causes more stress and is representative of many realistic shadows that may be seen in service, so we perform partial shade testing using a mask that covers 90% of the long dimension of the group of cells under stress.

Shadows cast by distant objects move across the face of a module throughout a day. Some kinds of obstructions, such as bird droppings, are periodically removed and redeposited in a new location. To replicate these effects, we apply stress using repeated applications of the critical mask, each time in a previously unstressed area.

In service, modules are connected in a series string that is loaded at the string's unshaded I_{mp}. Assuming the string of modules is long, a mask covering a small portion of a single module will not appreciably change this boundary condition. As such, we perform stress while the module is passing its own unshaded, pre-stress I_{mp}. This prevents stress-induced permanent changes to the module's I-V curve from changing the overall electrical boundary condition in an unrealistic manner. The test procedure is detailed in Section 3.3.

2.3 Light stabilization

Polycrystalline thin-film PV cells undergo reversible changes in performance upon exposure to light, sometimes called metastability. These changes can interfere with the proper quantification of the change in performance resulting from a stress test by masking the permanent change with a reversible one. We use a specific light-stabilization procedure, sometimes called light soaking, to eliminate the reversible change. The procedure is based upon the practices we have developed during research specifically targeting these effects[8] and is summarized in Section 3.1.

2.4 Computer simulation of partial shade stress

It is not generally possible to measure the internal thermal and electrical state of a PV module. The large-scale, interconnected nature of a thin-film PV module leads to nonintuitive behavior under nonuniform illumination. We have developed a computer model describing the two-dimensional electrical and three-dimensional thermal response of a module to nonuniform illumination. This model is the focus of a recent publication[5] and here we present some results that reinforce our testing approach.

3. TEST PROCEDURE

3.1 Light stabilization

To ensure that no reversible, light-induced change in P_{mp} is mistaken for a permanent, stress-induced change, we use a light stabilization procedure before performing flash I-V curve measurements:

1. Place modules in a class BBA light-exposure chamber
2. Expose modules to light under specific conditions:
   (a) 1000 Wm^{-2} irradiance
   (b) 50°C back-of-module temperature
   (c) Active maximum power point tracking
   (d) In situ I-V curve measurements every five minutes
3. Stop exposure when both stability criteria are met:
   (a) Light exposure duration exceeds 20 h

(b) A linear fit to the last 20 h of in situ P_{mp} measurements shows a slope of less than 1% per 20 h
4. Cool modules to 25°C
5. Perform a flash I-V curve measurement using a class AAA pulsed simulator between 30 min and 60 min after the end of the light exposure

3.2 Mask sizing

The objective of the mask sizing test is to determine the largest mask that results in nearly the maximum possible dissipated power per masked cell. We assume the dissipated power per cell is near the maximum when the module produces an I_{sc} larger than its unshaded, room-temperature I_{mp}, which we denote as $I_{mp,0}$. In a module that is badly shunted, this assumption may no longer be valid and a criterion based solely on room-temperature I_{sc} may be necessary. The procedure is:

1. Fabricate opaque masks in sizes appropriate to completely cover 5% to 30% of the cells in the module, in one-cell increments
2. Perform the light stabilization procedure and note the module's room-temperature $I_{mp,0}$
3. Collect an electroluminescence (EL) image
4. Apply the largest mask to an area in the center of the module
5. Perform a flash I-V measurement and note the module's masked I_{sc}, which should be below $I_{mp,0}$
6. Apply the next smaller mask to a subset of the cells covered by the previous mask
   · If the cell pitch is small, every other mask can be skipped until $I_{sc} > \frac{I_{mp,0}}{2}$ without changing the result
7. Perform a flash I-V measurement and note the module's masked I_{sc}
8. Repeat steps 6 and 7 until $I_{sc} > I_{mp,0}$
   · This occurs when the critical mask is in place
   · Note the size of the critical mask
9. Collect an EL image
   · If the EL image from step 9 shows new damage compared to the one from step 3, do not use the same module for stress testing

To prevent the module from relaxing to its pre-stabilized state during this operation, it should be performed as quickly as possible.

3.3 Partial shade stress

The objective of the partial shade stress test is to quantify the loss of power resulting from a sequence of shadows applied while the module is illuminated and passing current. The conditions are chosen to represent an adverse realistic case. The steps are:

1. Fabricate a version of the critical mask that is 90% opaque and will cover 90% of the long dimension of the masked cells
2. Perform the light stabilization procedure and note the module's pre-stress P_{mp}
3. Collect an EL image
4. With no mask applied, place the module in a light-exposure chamber under these conditions:
   (a) 1000 Wm^{-2} irradiance
   (b) 40°C to 60°C mean back-of-module temperature, measured using IR thermography
   (c) Active maximum power point tracking
5. When the module has thermally equilibrated (< 1°C change in 10 min), note its I_{mp} at this equilibrium temperature, denoted as $I_{mp,1}$, and use identical cooling conditions for subsequent steps
6. Change the module's electrical loading condition to V_{oc}
7. Apply the mask from step 1 to the module
   · To perform this step it may be necessary to briefly remove the module from the chamber
8. Allow five to ten minutes for thermal equilibration
9. Apply stress by changing the electrical loading condition to a constant current of $I_{mp,1}$ for ten minutes
   · The current-loading condition can be periodically reduced $0.95I_{mp,1}$ to act as excitation for lock-in thermography
10. Change the module's electrical loading condition to V_{oc}

11. Move the mask to an area of the module that is at least two cell pitches away from any previously stressed area
    · To perform this step it may be necessary to briefly remove the module from the chamber
12. Repeat steps 8 through 11 until at least 50% of the cells in the module have been stressed
13. Perform the light stabilization procedure and note the module's post-stress P_{mp}, comparing it to the measurement taken in step 2
14. Collect an EL image, comparing it to the image collected in step 3

4. METHOD

4.1 Computer simulation of partial shade stress

Our modeling and simulation approach is described in detail elsewhere.[5] Briefly, we simulated the steady-state coupled heat transfer and electrical continuity problem of monolithic CIGS modules. The front and back contacts were simulated in two dimensions and the PV cell was included as a current source in one contact and an equal current sink in the other contact. We used a physics-based compact model to describe the PV cell's temperature-, irradiance- and voltage-dependent current density.[6]

The temperature in the module package was simulated using a three-dimensional model of a glass-encapsulant-glass module. The electrically dissipated heat was included as a heat source on the front surface of the module's back glass. A convection boundary condition was applied to the exterior surfaces of the module.

The thermal and electrical models were fully coupled and were solved simultaneously: heat dissipated by the PV device was delivered to the module package and the temperature inside the module package was used in the temperature-dependent PV cell model.

This modeling framework enabled the simulation of nonuniform patterns of illumination, including those used for shade stress tests. To show the details of voltage and temperature in a realistic module, we simulated a 100-cell, 2,500 cm^2 (0.5 m$\times$0.5 m) module. The module was loaded at its unshaded I_{mp} for its operating temperature in 25°C ambient conditions, which was approximately 50°C. We simulated the steady-state temperature and voltage response resulting from the application of a 90% opaque mask covering 90% of the long dimension of the masked cells. The mask covered eight cells, determined in a separate simulation to be this module's critical mask size.

To evaluate hundreds of combinations of mask opacity and extent, we simulated a 20-cell, 100 cm^2 (0.1 m $\times$ 0.1 m) mini-module. In this mini-module, the critical mask covered two cells and we simulated versions of the critical mask ranging in opacity from 0.0 to 1.0 (blocking 0% to 100% of incident light) and ranging in extent from 0% to 100% of the long dimension of the masked cells. The mini-module was loaded at its unshaded, operating-temperature I_{mp} for each of these simulations. We determined the peak temperature, current density and reverse voltage for each of the simulated conditions.

4.2 Partial shade stress test

On three types of commercial monolithic CIGS modules, designated as type A, type B and type C, we applied the test procedure detailed in Sections 3.1–3.3. We excluded the module used in the mask sizing test from future tests, so a total of six modules were used. We completed the mask sizing test in $<$ 1 h for each module.

Continuous light exposures for both stabilization and stress were performed in a chamber with 52 metal halide lamps and closed-loop control of back-of-module temperature and of light intensity. During light stabilization the modules were cooled by circulating room air through the chamber and module temperature was measured with a thermocouple at the center of the module. During partial shade stress we cooled modules using either a fixed air knife or natural convection and temperature was measured using an InSb IR camera.

Pulsed I-V measurements were performed on a long-pulse solar simulator. EL images were collected using an InGaAs camera in room light and with background subtraction.

5. RESULTS AND DISCUSSION

In these results, we have cropped EL and IR images and normalized voltage and current measurements.

5.1 Computer simulation of partial shade stress

The mask, simulated voltage map and simulated temperature map for the 100-cell, 2,500 cm^2 module are shown in Figure 1. Note that the right-most 10% of the masked cells was illuminated, but still nearly as far in reverse bias as the masked 90% of those cells. This partial illumination of the masked cells resulted in current crowding, as described above, which led to high device temperature in the illuminated region of the masked cells.

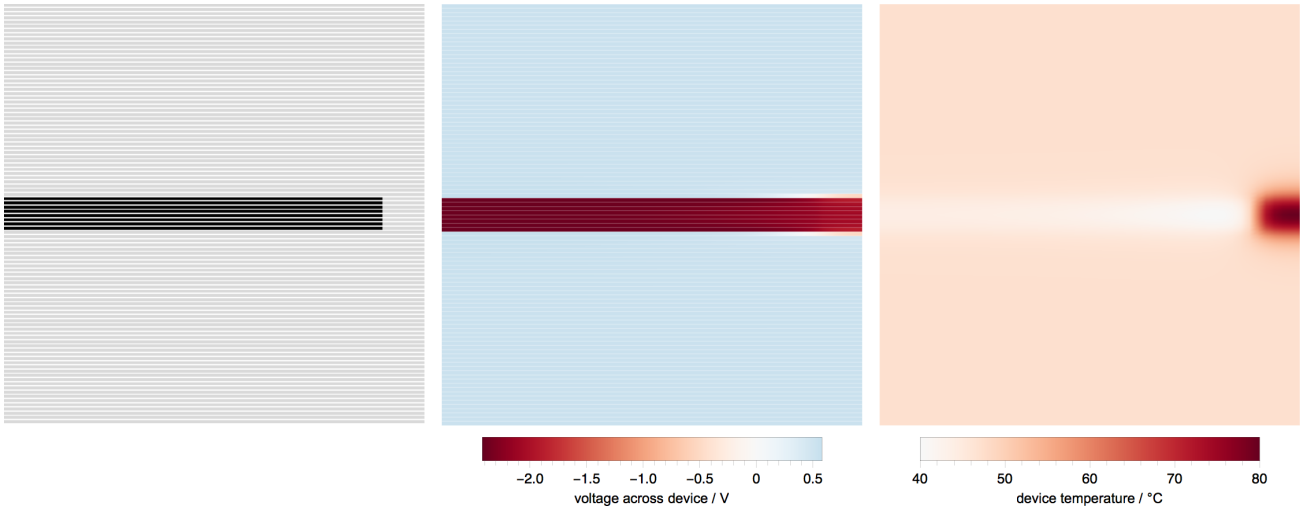

Figure 1. Mask schematic (left), simulated voltage map (center) and simulated device temperature map (right) for the 100-cell module with a 90% opaque, 90% extent mask. In the mask schematic, the black areas show the location of the mask. The horizontal white lines illustrate the locations of the scribe lines. The simulated voltage map shows that the entire extent of the masked cells was driven far into reverse bias, including the unmasked portions. The temperature map shows that current crowding and incident light led to a patch of high temperature in the illuminated area.

This result illustrates that leaving a portion of the masked cells exposed to light, consistent with many kinds of shadow experienced in service, places additional stress on this illuminated portion. Using a partial-extent mask for stress testing helps to expose any issues associated with short-term degradation of packaging materials due to a patch of high temperature.

The maximum temperature, current density and reverse voltage for the mini-module under various masking conditions are shown in Figure 2. For clarity, only results from the the 100% and 90% extent masks are plotted. The maximum temperature plot reflects the current crowding result shown in Figure 1, motivating the use of a partial-extent mask for applying heat to a patch of the module packaging materials. The maximum current density plot shows the high current density that resulted from from current crowding and incident light adjacent to the partial-extent mask. This motivates the use of a partial-extent mask for exciting current-density-driven failures.

The maximum reverse voltage plot illustrates that the maximum reverse voltage in the module was nearly the same for a full-extent and a partial-extent mask. This voltage is the driving force for the formation of shunts in weak areas of the module and, following their formation, it is the driving force for very high local current flow and power dissipation in these shunts. This result shows that the partial-extent mask does not compromise reverse voltage stress.

Figure 2 also shows the high sensitivity of stress to the exact amount of light reaching cells behind an opaque or nearly-opaque mask. This sensitivity is due to LERB. Combined with the fact that a realistic obstruction never blocks 100% of light reaching the PV device, this motivates the selection of a partially opaque mask for stress testing. The sensitivity of stress to opacity is much less at 90% opacity, a realistic figure for a real obstruction and the opacity we use for partial shade stress testing.

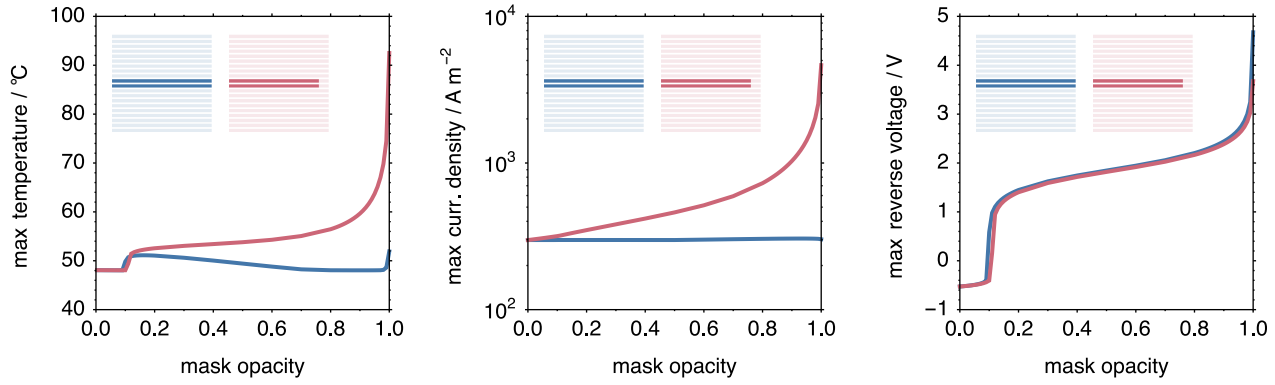

Figure 2. Simulated maximum temperature (left), current density (center) and reverse voltage (right) as a function of mask opacity (x axis) and mask extent in the mini-module. Mask extent is illustrated in the inset schematics. The blue lines and schematic are for a 100% extent mask and the red lines and schematic are for a 90% extent mask. Each of these three driving forces for failure was approximately equal or greater with the partial-extent mask. The sensitivity of stress to mask opacity is very high for nearly opaque masks.

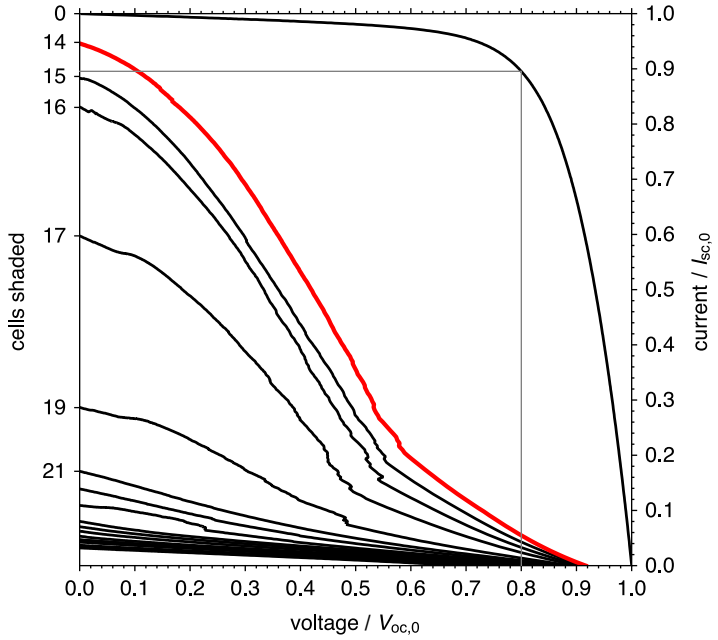

Figure 3. I-V curve measurements collected during the mask sizing procedure for one of the three modules tested. Voltage and current are normalized to the V_{oc} and I_{sc} of the unmasked module, denoted as $V_{oc,0}$ and $I_{sc,0}$. The critical mask was 14 cells for this module and the associated I-V curve is highlighted in red. The gray lines indicate the module's unmasked I_{mp} and V_{mp}.

5.2 Mask sizing

Normalized I-V curves measured as a part of the mask sizing test for one of the modules are shown in Figure 3. On this module, I_{sc} exceeded $I_{mp,0}$ when the 14-cell mask was applied. Our use of the shrinking-mask approach means that no mask smaller than the critical mask was applied. Jagged artifacts appear in some of the I-V curves in Figure 3. These result from the formation of shunts during the I-V measurement.

For the module types we tested, the use of the largest mask where $I_{sc} > I_{mp,0}$ resulted in a power dissipation

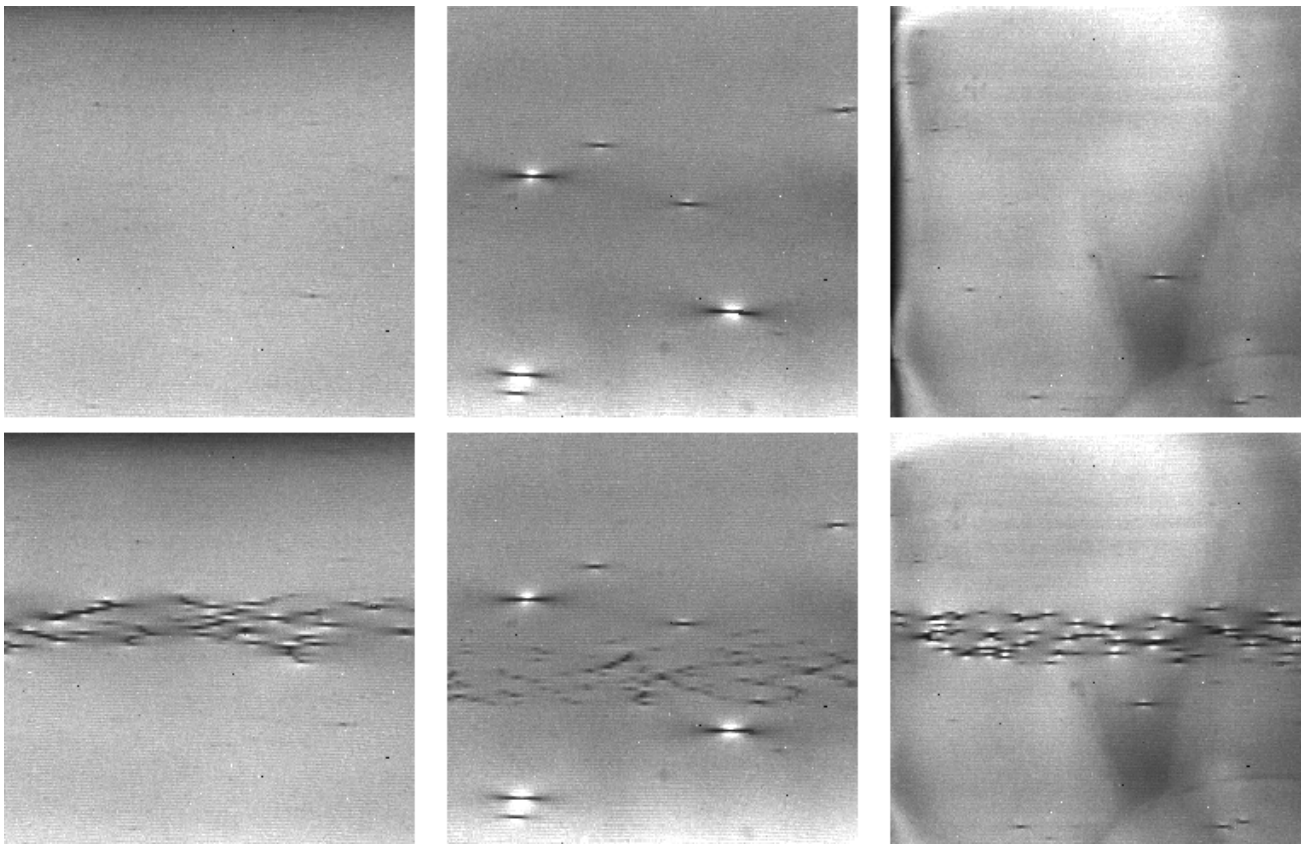

Figure 4. EL images from modules of type A (left), type B (center) and type C (right) from before (top) and after (bottom) the mask sizing procedure. Horizontal bands of black spots appear in the "after" images, indicating the formation of many shunts during masked exposure to pulsed light.

in each masked cell of $> 90\%$ of the maximum possible power dissipation. This is because in these modules, $I_{\mathrm{mp}} \approx 0.9 I_{\mathrm{sc}}$ under uniform illumination. A criterion based solely on I_{sc} may be preferable to accommodate modules with lower shunt resistance and the resulting smaller $\frac{I_{\mathrm{mp}}}{I_{\mathrm{sc}}}$ ratio.

Cropped EL images from before and after the mask sizing test are shown in Figure 4. In these images, scribe lines are oriented horizontally. In all three modules, a horizontal band of black spots indicates that dozens of new shunts formed as a result of fewer than twenty ~ 100 ms pulses of light at room temperature. This suggests that this type of damage may happen practically instantaneously. If this shunting is the only kind of damage of interest, an abbreviated test using only a flash simulator may be possible. The barriers to development of such a test include differences in the nature of the light pulse and electrical loading used by different types and configurations of flash simulators.

In this work we excluded the modules used for the mask sizing test from subsequent tests, instead using previously unstressed modules of identical type. It may be possible to use a single module by carefully accounting for the damage that occurred during the mask sizing test and the effect on subsequent steps.

5.3 Partial shade stress

Normalized I-V curves from before and after the full partial shade stress procedure are shown in Figure 5. The curves show that all three module types experienced a loss of performance due to fill factor and voltage reductions. These observations are consistent with heavy shunting resulting from reverse bias. Light-stabilized measurements show that module type A lost 6.1%, type B lost 11.4% and type C lost 4.2% in P_{mp}.

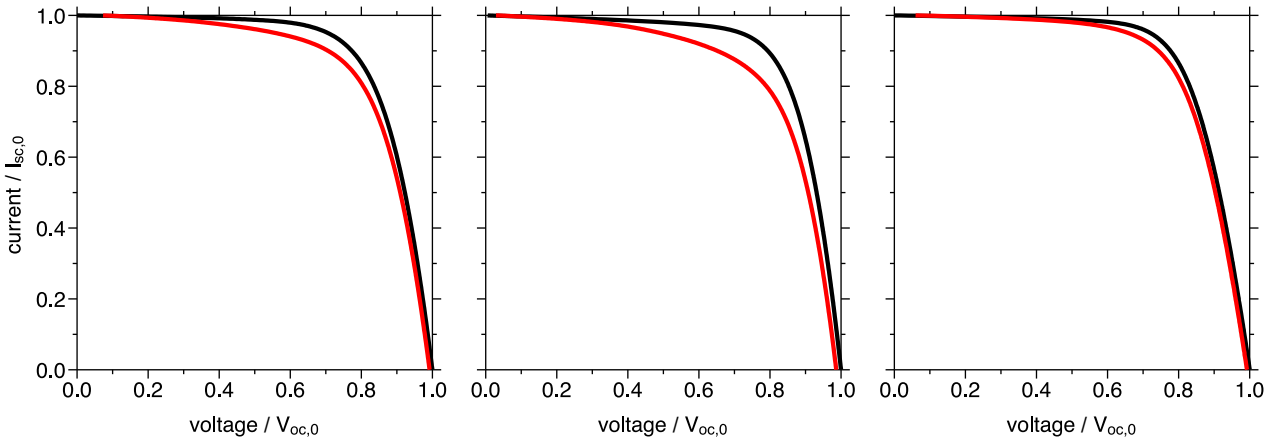

Figure 5. I-V curves from before (black) and after (red) the partial shade stress test for module type A (left), type B (center) and type C (right). Voltage and current are normalized to the V_{oc} and I_{sc} of the unmasked module, denoted as $V_{oc,0}$ and $I_{sc,0}$.

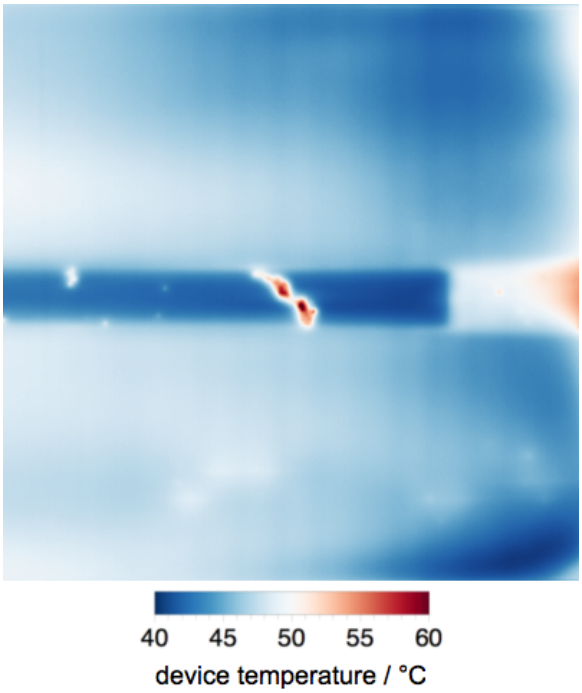

Figure 6. Cropped temperature map of the back surface of a masked, illuminated module. The cool, horizontal rectangle in the center of the image is the masked area. The hot patch to the right of this rectangle is the illuminated area, heated by crowded current. The hot spots in the masked area are shunts that appeared during the test.

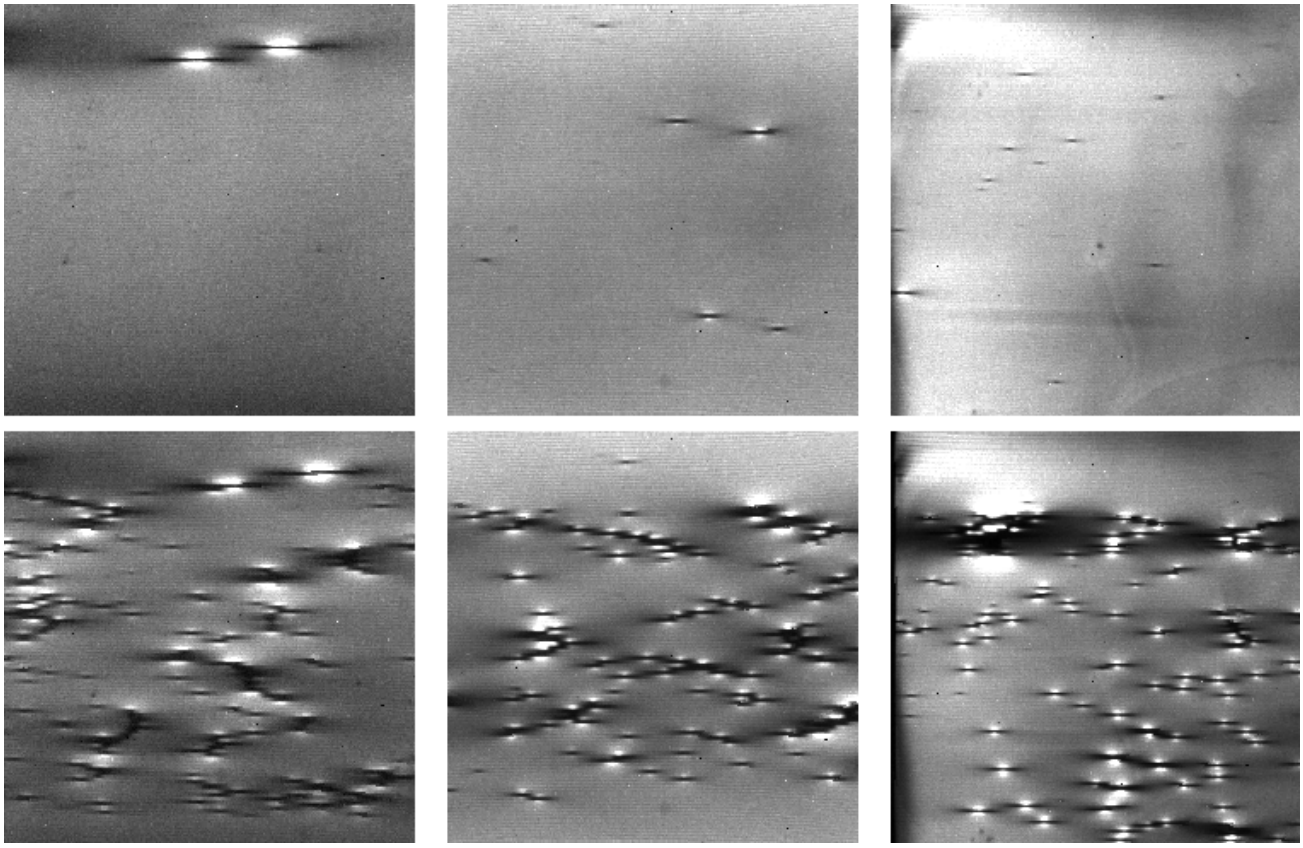

Figure 7. EL images from before (top) and after (bottom) the partial shade stress test for module type A (left), type B (center) and type C (right). The horizontal bands of black spots indicate heavy shunting as a result of partial shade under continuous illumination.

A cropped temperature map, measured with IR thermography from the back surface of an illuminated module during the partial shade stress test, is shown in Figure 6. The scribe lines are oriented horizontally and the masked area is visible as a cool, horizontal rectangle in the center of the image. The illuminated portion of the masked cells is at the right side of the image and shows heating due to current crowding and incident light, consistent with the simulated temperature result in Figure 1. Unlike in the simulation, which considered a module with uniform junction characteristics, the experimental temperature map shows localized hot spots underneath the mask. These are coincident with shunts that formed as a result of reverse bias during the test. These spots appeared immediately when the loading condition was switched from V_{oc} to $I_{\mathrm{mp},1}$.

Cropped EL images of modules before and after the partial shade stress test are shown in Figure 7. Each module type shows a similar pattern of heavy shunting in the areas that were masked during the test. New shunts in these images are coincident with a visible feature: a thin, gray streak, sometimes serpentine or branched and often ending near a scribe. This feature cannot always be photographed easily through textured glass, but typical examples are shown in Figure 8. These features are consistent with those observed in previous work on reverse bias damage in CIGS.[9] However, these features are not considered major visual defects according to IEC 61646 and would not lead to a failure of the standard test.[1]

5.4 Light stabilization

We performed room-temperature pulsed I-V measurements both immediately after stress and after post-stress light stabilization. In each module type, we observed a change in the P_{mp} loss upon stabilization. In type B the damage became worse and in types A and C it stayed the same or recovered slightly. Note that to apply the mask to $\geq 50\%$ of cells in module type B required two sessions, between which we performed the light-stabilization

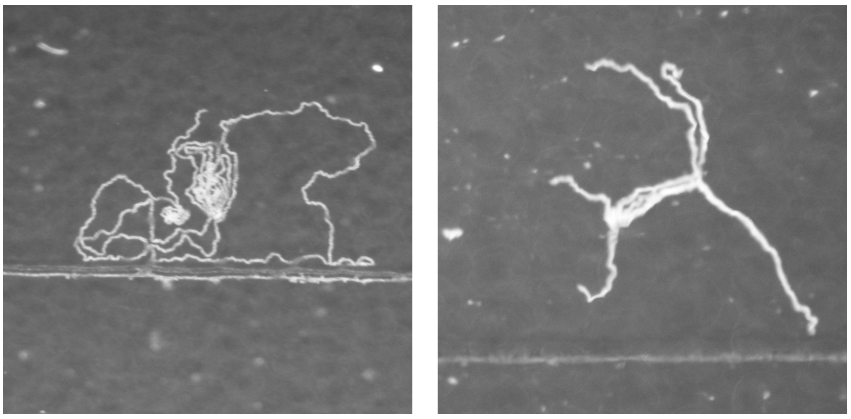

Figure 8. Visible light images of defects typical of those coincident with dark spots in EL images. The left image covers an area about 8 mm wide and the right image covers an area about 5 mm wide.

procedure. The results, summarized in Table 1, reinforce the need to perform light stabilization both before and after partial shade stress, even though the stress occurs under continuous illumination.

Table 1. Loss of P_{mp} due to the partial shade stress test for the three module types. Type B was stressed in two phases with an intermediate light stabilization.

type A	
state	P_{mp} loss
baseline (light stabilized)	0.0%
immediately after stress	6.5%
light stabilized	6.1%
type B	
state	P_{mp} loss
baseline (light stabilized)	0.0%
immediately after first stress phase	7.0%
light stabilized	9.5%
immediately after second stress phase	10.5%
light stabilized	11.4%
type C	
state	P_{mp} loss
baseline (light stabilized)	0.0%
immediately after stress	4.7%
light stabilized	4.2%

6. CONCLUSION

We have introduced a test procedure for quantifying a monolithic PV module's robustness to partial shade stress. The test procedure moves beyond the standard hot spot endurance test by carefully quantifying the loss in performance resulting from stress and by using adverse but realistic shading and loading conditions. The choice of shading conditions used for stress, namely repeated application of a 90% opaque, 90% extent mask, was guided by consideration of realistic shading scenarios and reinforced by results from computer simulations. Measurements of performance loss are made after the application of a strict light-stabilization process, avoiding the effects of reversible performance changes.

We applied the partial shade test to three commercial CIGS modules from different manufacturers. Every module suffered permanent damage during masked flash testing totaling < 2 s of light exposure. We continued

with a previously unstressed module to prevent this damage from interfering with subsequent stages of the test. With careful planning, it may be possible to use a single module for the entire test. During the stress portion of the test, each module lost 4%–11% in P_{mp} due to the widespread formation of localized shunts in the masked areas. Despite our use of a partial-extent mask, which causes an entire patch of the module to operate at elevated temperature, we observed no degradation of encapsulation materials or other major visual defects, which the standard hot spot endurance test is designed to precipitate. In one module, exposure to uniform light after stress caused the loss in P_{mp} to worsen and in others the loss stayed the same or recovered slightly. This reinforces the need to perform light stabilization before making initial and final performance measurements.

The partial shade test procedure we have demonstrated here can serve as a starting point for the development of comparative tests that help guide technology development. With the addition of pass/fail criteria it can also serve as a starting point for qualification tests that screen for faulty product designs.

ACKNOWLEDGMENTS

This work was supported by the U.S. Department of Energy under Contract No. DE-AC36-08GO28308 with the National Renewable Energy Laboratory. Some of the data in this report were obtained using equipment at the Energy Systems Integration Facility (a national user facility sponsored by the U.S. DOE Office of Energy Efficiency and Renewable Energy) located at the National Renewable Energy Laboratory. The U.S. Government retains and the publisher, by accepting the article for publication, acknowledges that the U.S. Government retains a nonexclusive, paid up, irrevocable, worldwide license to publish or reproduce the published form of this work, or allow others to do so, for U.S. Government purposes.

REFERENCES

[1] IEC 61646, "Thin-film terrestrial photovoltaic (PV) modules: Design qualification and type approval - edition 2.0," IEC standard (2008).

[2] Mack, P., Walter, T., Kniese, R., Hariskos, D., and Schäffler, R., "Reverse bias and reverse currents in CIGS thin film solar cells and modules," in [*23rd European Photovoltaic Solar Energy Conference and Exhibition*], (2008).

[3] Szaniawski, P., Lindahl, J., Törndahl, T., Zimmermann, U., and Edoff, M., "Light-enhanced reverse breakdown in Cu(In,Ga)Se2 solar cells," *Thin Solid Films* **535**(0), 326 – 330 (2013).

[4] Puttnins, S., Jander, S., Pelz, K., Heinker, S., Daume, F., Rahm, A., Braun, A., and Grundmann, M., "The influence of front contact and buffer layer properties on CIGSe solar cell breakdown characteristics," in [*26th European Photovoltaic Solar Energy Conference and Exhibition*], (2014).

[5] Silverman, T. J., Deceglie, M. G., Sun, X., Garris, R. L., Alam, M., Deline, C., and Kurtz, S., "Thermal and electrical effects of partial shade in monolithic thin-film photovoltaic modules," *IEEE Journal of Photovoltaics* (in review) (2015).

[6] Sun, X., Raguse, J., Silverman, T. J., Deline, C., and Alam, M., "A physics-based compact model for CIGS and CdTe solar cells: from voltage-dependent carrier collection to light-enhanced reverse breakdown," in [*42nd IEEE Photovoltaics Specialists Conference (PVSC)*], (June 2015).

[7] Dongaonkar, S., Deline, C., and Alam, M., "Performance and reliability implications of two-dimensional shading in monolithic thin-film photovoltaic modules," *Photovoltaics, IEEE Journal of* **3**, 1367–1375 (Oct 2013).

[8] Deceglie, M. G., Silverman, T. J., Marion, B., and Kurtz, S., "Robust measurement of thin-film photovoltaic modules exhibiting light-induced transients," in [*Proceedings of the SPIE*], (submitted) (2015).

[9] Westin, P. O., Zimmermann, U., Stolt, L., and Edoff, M., "Reverse bias damage in CIGS modules," in [*24th European Photovoltaic Solar Energy Conference and Exhibition*], 2967–2970 (2009).